Eur Radiol (2009) 19: 845–856
DOI 10.1007/s00330-008-1214-4

CARDIAC

Christian Thilo
U. Joseph Schoepf
Leonie Gordon
Salvatore Chiaramida
Jill Serguson
Philip Costello

Integrated assessment of coronary anatomy and myocardial perfusion using a retractable SPECT camera combined with 64-slice CT: initial experience

Received: 28 May 2008
Revised: 22 August 2008
Accepted: 2 September 2008
Published online: 30 October 2008

This study received research support from Siemens Medical Solutions (Malvern, Pa). UJS is a medical consultant to Bayer, Bracco, General Electric, Siemens, and TeraRecon and receives research support from Bayer, Bracco, General Electric, Medrad, and Siemens. LG is a medical consultant to Cytogen Corporation. PC is a medical consultant to Bracco and receives research support from Siemens.

C. Thilo · U. J. Schoepf (✉) ·
L. Gordon · J. Serguson · P. Costello
Department of Radiology,
Medical University of South Carolina,
169 Ashley Avenue,
Charleston, SC 29425, USA
e-mail: SCHOEPF@MUSC.EDU
Tel.: +1-843-7922633
Fax: +1-843-7920409

C. Thilo · U. J. Schoepf · S. Chiaramida
Division of Cardiology,
Department of Medicine,
Medical University of South Carolina,
169 Ashley Avenue,
Charleston, SC 29425, USA

Abstract We evaluated a prototype SPECT system integrated with multidetector row CT (MDCT) for obtaining complementary information on coronary anatomy and hemodynamic lesion significance. Twenty-five consecutive patients with known or suspected coronary artery disease (CAD) underwent routine SPECT myocardial perfusion imaging (MPI). All patients also underwent repeat MPI with a mobile SPECT unit which could be attached to a 64-slice MDCT system. Coronary CT angiography (cCTA) was performed without repositioning the patient. Investigational MPI was compared with routine MPI for detection of myocardial perfusion defects (PD). Two observers diagnosed presence or absence of CAD based on MPI alone, cCTA alone, and based on combined MPI and cCTA with fused image display. In 22/24 patients investigative MPI corresponded with routine MPI (r=0.80). Stenosis ≥ 50% at cCTA was detected in 6/24 patients. Six out of 24 patients had PD at regular MPI. Three of these six patients had no significant stenosis at cCTA. Three out of 19 patients with normal MPI studies had significant stenosis at cCTA. Our initial experience indicates that the integration of SPECT MPI with cCTA is technically feasible and enables the comprehensive evaluation of coronary artery anatomy and myocardial perfusion with a single instrumental setup.

Keywords Image fusion · 64-slice CT · Myocardial perfusion imaging · Coronary artery disease

Introduction

Over the last decade, with the introduction of multidetector row CT (MDCT) and the development of advanced electrocardiography (ECG)-synchronized image acquisition and reconstruction techniques, coronary CT angiography (cCTA) has been validated as a valuable tool to diagnose coronary artery disease [1–7]. With 64-slice CT, the diagnostic performance has been significantly improved [1–7] over previous instrument generations. The enhanced assessment of coronary arterial wall lesions and tools relating these to acute and chronic changes in

myocardial perfusion is of increasing interest [8]. Despite all efforts, cCTA has limitations in the evaluation of stenosis severity as the positive predictive value of cCTA for identifying coronary stenoses causing ischemia is poor [9–11].

Myocardial perfusion imaging (MPI) using single photon emission computed tomography (SPECT) is the most widely used noninvasive imaging test to determine the hemodynamic significance of coronary artery disease and helps in the selection of patients requiring cardiac catheterization [12–16]. Annually, approximately 9.3 million MPI procedures are performed in the USA [17]. Newer investigations such as MRI and positron emission tomography (PET) may offer certain advantages over SPECT but have not yet been widely accepted [18, 19].

It has been reported that image fusion from independent SPECT and CT offers an incremental diagnostic value by integrating both sets of data [20]; however, this approach requires dedicated nonrigid image fusion algorithms [20, 21] since the studies are not acquired simultaneously. Visual techniques have been shown to be neither reproducible nor objective [22]. We evaluated a prototype retractable SPECT gamma camera integrated with a 64-slice multidetector CT system for obtaining complementary information on coronary artery stenosis and hemodynamic lesion severity with a single instrumental setup.

Materials and methods

Sources of support

This study was supported by a research grant provided by Siemens Medical Solutions (Hoffman Estates, IL). The authors had control of the data and information submitted for publication.

Study population

Our institutional review board approved this investigation and all patients signed written informed consent after they were given a thorough explanation of the study purpose and the involved risks, such as additional radiation exposure and drug administration during cCTA. All patients also consented to the use of their medical information for the purpose of this research project, in compliance with HIPAA (Health Insurance Portability and Accountability Act) requirements.

Between November 2006 and March 2007, 25 consecutive patients (Table 1) with known or suspected CAD and referred for clinically indicated MPI were prospectively enrolled. Exclusion criteria were: (a) unstable angina or vital signs; (b) creatinine level of more than 2.0 mg/dL (176.8 μmol/L); (c) pregnancy; and (d) known allergy to iodinated contrast material. Irregular heart rate, obesity, and heavy coronary calcifications were not considered exclusion criteria.

Table 1 Demographics of 25 patients referred for routine clinical rest/stress MPI

Demographic variable	Number	Percent
Patient age (years)		
Mean	60	
Range	33–80	
Patient sex		
Male	14	56
Female	11	44
Known CAD	12	48
CAD risk factors		
Hypertension	21	84
Hyperlipidemia	19	76
Smoking (current or former)	5	20
Type 2 diabetes	6	24
Family history of CAD	14	56
0 risk factors	0	
1–2 risk factors	7	
3–4 risk factors	16	
≥ 5 risk factors	2	
Chest pain evaluation		
Stable angina	16	64
Unstable angina	0	0
No angina	9	36
BMI (kg/m^2)	30 (±8 SD)	
< 25	5	20
25–30	11	44
> 30	9	36

CAD coronary artery disease, *BMI* body mass index, *SD* standard deviation

Routine clinical rest/stress SPECT MPI

All patients underwent a routine clinical 1-day, ECG-gated rest/stress protocol (Fig. 1). After fasting at least 4 h, 10 mCi (370 MBq) Tc sestamibi was administered intravenously at rest. After 45–50 min, images were obtained with a SPECT gamma camera system (Vertex™ V60, Philips, Best, The Netherlands) with the patient supine using a sequential acquisition with 32 stops. Data were recorded with attenuation correction using a gadolinium source [23]. Patients were then stressed and injected with 30 mCi (1,110 MBq) Tc sestamibi at peak stress. Patients were imaged 40-min post-stress using the same gamma camera and acquisition protocol.

Twenty patients (n=20) were stressed on a treadmill utilizing the Bruce protocol. Five patients who were unable to exercise had pharmacologic stress with adenosine (140 mcg/kg/min for 4 min).

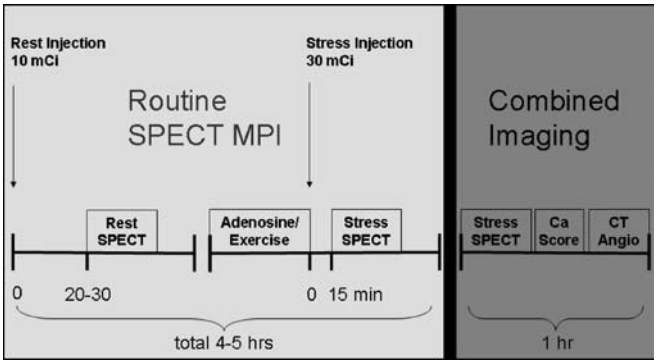

Fig. 1 Routine clinical 1-day Tc-tetrofosmin SPECT MPI protocol (*light gray*) and investigative CT/SPECT protocol (*dark gray*). Combined imaging includes repeat acquisition of stress images with SPECT camera attached to a 64-slice CT system for coronary calcium scoring (Ca score) and coronary CT angiography (CT angio)

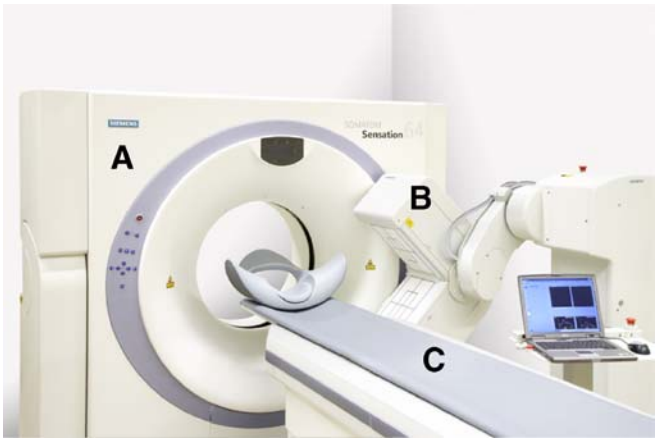

Fig. 2 Integrated instrumental setup of a 64-slice MDCT system (*A*) with a retractable SPECT camera (*B*) which can be attached to the CT patient table (*C*) from its storage position when active via a rail-track (not visible) in the room floor

After processing and reconstruction, the ECG-gated images were analyzed by two experienced readers in consensus, both with more than 10 years of experience in nuclear cardiology, using a commercially available software package (Cedars QGS/QPS; Cedars-Sinai Medical Center, Los Angeles, CA). Images were analyzed for the relative activity in each section of the myocardium. Interpretation included evaluation of perfusion defects with and without attenuation correction, wall motion, and ejection fraction. Perfusion defects were classified as reversible (ischemia) or fixed (scar). A very small fixed perfusion defect with normal regional wall motion on gated SPECT was considered an artifact rather than a scar [24]. Anterior and septal perfusion defects were allocated to the left anterior descending coronary artery (LAD), lateral defects to the left circumflex coronary artery (LCX), and inferior defects to the right coronary artery (RCA) according to current conventions [25]. Quantification was performed from the polar map plot and any value of 2 standard deviations or above was considered significant. Between 1 and 2 standard deviations findings were correlated with clinical presentation on stress test and with ECG.

Combined imaging using SPECT MPI, CT calcium scoring, and cCTA (CT/SPECT)

Immediately after completion of the routine clinical rest/stress SPECT study, patients were transferred to the CT suite to be examined with an integrated cardiovascular CT/SPECT setup (Fig. 2) consisting of a 64-slice CT system (SOMATOM Sensation Cardiac, Siemens, Forchheim, Germany) and a retractable prototype SPECT camera (Siemens, Hoffman Estates, IL) which was attached to the CT patient table from its storage position when active via a rail-track in the room floor. The examination started with repeat SPECT imaging for approximately 30 min after completion of the routine MPI examination. Immediately afterwards, a non-contrast-medium-enhanced study for the evaluation of coronary calcium was performed in all patients while they remained in the same position on the CT table by using the following parameters: 120 kV, 150 mAs, 0.33-s rotation time, 1.2-mm collimation, and 3.0-mm reconstructed section thickness with 50% overlap. One observer calculated the total Agatston and volume score using a dedicated workstation (Multi Modality Workplace; Siemens). Non-contrast-medium-enhanced calcium scoring derived anatomic maps were used to correct for photon attenuation and scatter, minimizing soft tissue attenuation artefacts and allowing for better detection of true myocardial perfusion defects. Lastly, retrospectively ECG-gated, contrast-medium-enhanced cCTA was performed in each patient by using the following parameters: 120 kV, 900 mAs, 0.33-s rotation time, 0.6-mm collimation, *z*-flying focal spot technique, and pitch of 0.2. Patients with average heart rates greater than 65 bpm and no contraindications to the use of beta-blockers received up to three intravenous injections of 5 mg (up to 15 mg total) of metoprolol tartrate (Lopressor; Novartis, East Hanover, NJ) immediately prior to the CT examination.

Image acquisition was begun regardless of the eventual heart rate achieved after metoprolol injection. In the absence of contraindications (hypotension, current use of nitrate medications, migraine sensitive to nitrates) patients were given a 0.4-mg nitroglycerin tablet (NitroQuick; Ethex, St Louis, Mo) sublingually 2 min before the start of image acquisition. CT studies were acquired in a caudocranial direction with simultaneous recording of the patient's ECG signal to enable retrospective registration of image reconstruction to the desired cardiac phase. The examination range extended from the level of the carina to just below the diaphragm. Delay time was determined by

injection of a 20-mL contrast medium test bolus at 5 mL/s, followed by 50 mL saline, using a dual-syringe injector (Stellant D; Medrad, Indianola, PA). The peak time of test bolus enhancement in a region of interest in the ascending aorta was used as the delay time.

Arterial enhancement was achieved with 50–75 mL of a nonionic contrast medium (iopamidol; Isovue 370 mgI/mL, Bracco, Princeton, NJ) infused through an 18-gauge intravenous antecubital catheter at 5 mL/s, followed by a 50 mL saline chaser bolus. The contrast agent volume was individually computed according to the following formula: $V = T \times 5$, where V is the volume in milliliters and T is the examination time in seconds. Image reconstruction was performed using single-segment reconstruction and retrospective ECG gating [26–28]. Reconstruction intervals relative to the R–R interval (percentage R–R interval) with the least cardiac motion were determined on the basis of a preview series consisting of 20 images reconstructed at 20 different R–R interval positions in 5% increments (0–95%) at the same z-position at the midlevel of the heart. Image reconstruction parameters comprised an individually adapted field of view encompassing the heart, a medium soft-tissue convolution kernel, and a section thickness of 0.75 mm with an increment of 0.3 mm. The room time for combined MPI and CT was recorded and compared with the routine clinical rest/stress SPECT study.

Image evaluation was performed on a 3D enabled workstation (Multi Modality Workplace; Siemens) with a standardized window level of 100 HU and window width of 700 HU. Images for each patient were independently analyzed by two cardiovascular radiologists, both with more than 8 years of experience reading coronary multidetector row CT images. Readers were blinded to the patient's clinical data. They were asked to rate the quality of vessel visualization and to identify and grade stenosis in each patient including the tissue composition of causative lesions. Incidental findings with possible impact on patient management were recorded. Transverse sections, multiplanar reformations, and thin-slab maximum intensity projections (5 mm) were used for image display. In addition, stenosis severity was assessed using dedicated cardiac CT visualization software (Circulation; Siemens) which automatically extracts the coronary artery vessel tree from the contrast-medium-enhanced data set and subsequently displays a particular vessel as a curved multiplanar reformation (cMPR) along its centerline. With this tool, the degree of stenosis is evaluated by applying a semiautomated measuring tool to the automatically generated cMPRs. In the case of discrepancies between the observers, measurements were repeated and the results were analyzed in consensus. The extent of CAD was classified as follows: (a) no signs of atherosclerosis, (b) atherosclerosis with stenosis of 49% or less, (c) 50–69% stenosis, (d) 70–99% stenosis, and (e) total occlusion. Wherever available, findings at cCTA were compared with clinically indicated coronary catheterization.

Image fusion

Immediately after the hybrid CT/SPECT acquisition, raw data were assessed for motion to provide the ability to motion correct the data. Subsequently, the SPECT and CT attenuation correction data were processed to display corrected and uncorrected gated perfusion. After aligning the myocardial outlines of SPECT MPI and cCTA, fused volume rendered images were automatically generated. Alignment of the two fields of view (CT and SPECT) required six variables, three translations (dx, dy, and dz) and three rotations (rx, ry and rz); with z as the axis the CT rotates about, x as lateral, and y as vertical. The SPECT component was aligned in rx, ry, rz, and dx, and the fusion software was utilized to align the dy and dz data sets. The CT/SPECT images were reviewed by two different, blinded, experienced readers unaware of the routine MPI results applying the same parameters used at routine MPI reading. As a first step, attenuation- and non-attenuation-corrected images were examined for image quality and perfusion defects. Subsequently, fused images were evaluated and compared with investigational SPECT images and CTA.

Statistical analysis

Statistical analysis was performed with Sigma Stat 3.5, Sample Power 2.0 (SPSS, Chicago, IL) and Medcalc 9.3.2.0 (Mariakerke, Belgium). Descriptive statistics measures included frequency, mean, standard deviation, minimum, and maximum stratified by age, sex, BMI, degree of stenosis, Agatston scores, and volume.

A generalized estimating equation (GEE) was not utilized for calculating sensitivity, specificity, and accuracy due to the fact there was no true independent reference standard. Reader-specific values were compared using the McNemar test. Kappa (κ) analysis was used to determine agreement for the diagnosis of significant perfusion defects on the basis of regular and investigative MPI.

Estimates of power (85%) indicated a sample of 25 participants was sufficient to detect a kappa coefficient of 0.025.

Results

Table 1 summarizes patients' characteristics. Out of 25 patients, 24 were successfully imaged using all modalities. One patient prematurely aborted the research portion of the investigation due to back pain and was excluded from further analysis. Integrated assessment with SPECT MPI and CT using the investigational instrumental setup averaged 1-h total room time.

Routine clinical rest/stress SPECT MPI findings

Routine clinical SPECT MPI revealed perfusion defects in 6/24 patients (3 fixed and 6 reversible defects). Two defects were located in the anterior, one in the apical, one in the septal, one in the lateral, and four in the inferior territory. All other patients were deemed to have normal myocardial perfusion by the observers.

MPI findings using the investigational CT/SPECT system

Results at CT/SPECT MPI corresponded with diagnosis at routine clinical MPI in 22/24 patients (r=0.80). Image quality was rated as good or excellent in all patients. CT/SPECT MPI did not miss any of the perfusion defects detected at routine clinical MPI. In two patients additional perfusion defects were identified at CT/SPECT MPI that were not seen on routine clinical MPI.

CT findings using the CT/SPECT system

CT image quality was rated as good or excellent in 23 patients and was poor in 1 patient due to irregular heart rate. The mean Agatston score was 220±411 with a mean volume score of 193±358 mm^3 calcified tissue. Distribution of calcium scores is given in Fig. 3. One patient showed an Agatston score of 1,472. Image quality was poor in this patient but still diagnostic (same patient had irregular heart rate, see above). Coronary artery stenosis ≥ 50% was detected in six patients. In seven patients noncalcified lesions were identified; in four of these seven patients no stenosis ≥ 50% was present.

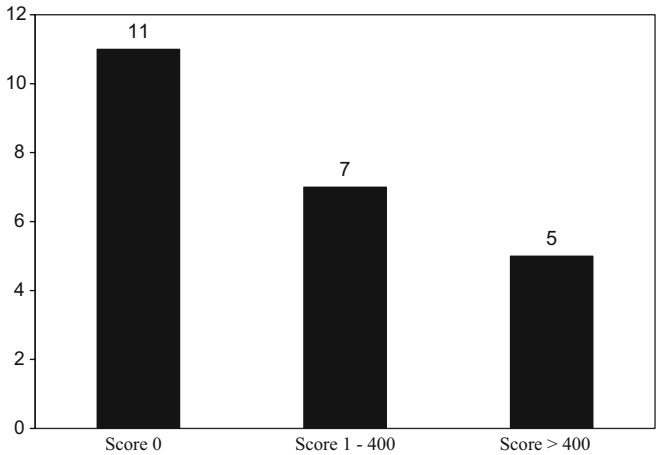

Fig. 3 Number of patients with Agatston scores of 0, 1–400, and >400, respectively. In two patients calcium scores were not obtained due to previous bypass surgery

Findings using cCTA and routine clinical MPI

On side-by-side analysis of routine clinical MPI and cCTA, three out of ten stenoses ≥ 50% (30%) matched with corresponding perfusion defects. On a per patient basis, three out of six patients with perfusion defects had significant stenosis at cCTA. Three out of 19 patients (16%) with < 50% stenosis at cCTA had perfusion defects at MPI. Three out of nineteen patients (16%) with normal routine clinical MPI studies had significant stenosis at cCTA, subsequently confirmed at catheter angiography. Four out of nineteen patients (21%) with normal routine clinical MPI had noncalcified plaque.

Findings using 3D fused images from CT/SPECT

Utilizing the 3D fused images, four out of ten (40%) stenoses ≥ 50% seen at cCTA had CT/SPECT MPI perfusion defects in their corresponding myocardial territory. Six perfusion abnormalities on fused images had no correlate at cCTA. In one patient (Fig. 4) a small apical perfusion defect was not appreciated by the observers, both on routine clinical SPECT MPI and on the isolated SPECT component of the CT/SPECT investigational system. cCTA in this patient showed significant LAD stenosis which was later confirmed by catheter angiography. On fused CT/SPECT display (Fig. 4), the perfusion defect can be more clearly visualized.

Figure 5 illustrates CT/SPECT findings in one patient (Table 2, patient 23) with known CAD, chronic, stable angina pectoris, and cardiovascular risk factors referred for MPI.

Comparison with coronary catheterization

Of the six patients with significant stenosis at cCTA, four underwent invasive coronary catheterization. In all four cases stenosis was confirmed and stent placement was performed in three patients (see Table 2; patient 1, stent placement LAD; patient 4, no stent placement because of chronic occlusion of RCA; patient 7, stent placement LAD; patient 13, stent placement CABG to RCA). In patient 21 with 50–60% stenosis at cCTA and only mild symptoms, medical therapy was recommended. The same regimen was prescribed in patient 23 with 50–60% stenosis with normal myocardial perfusion at both modalities.

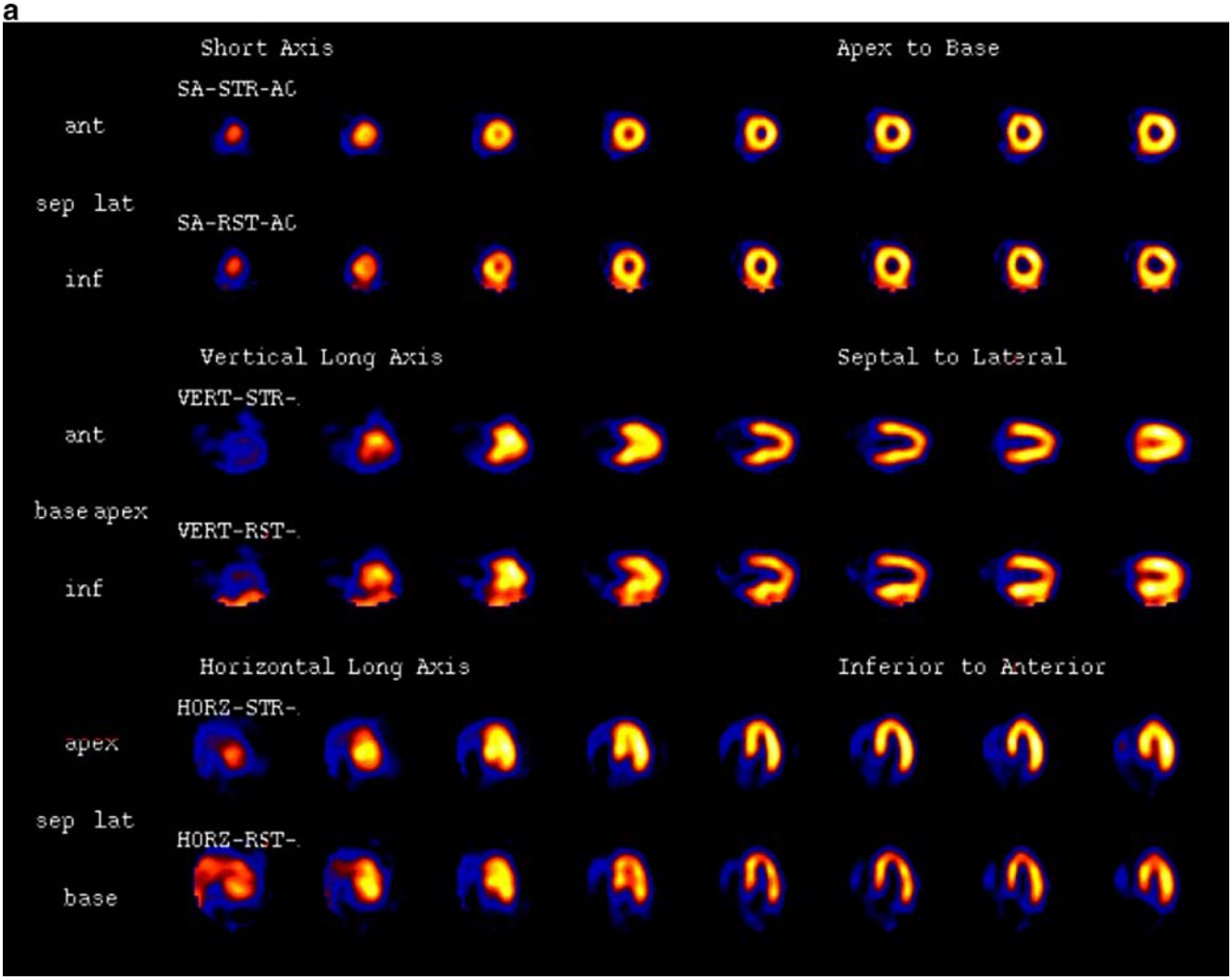

Fig. 4 Routine clinical SPECT MPI (**a**) and CT/SPECT (**b**) in a 55-year-old man (Table 2, patient 1) with typical exertional angina and cardiovascular risk factors clinically referred for myocardial perfusion imaging. The routine clinical SPECT MPI (**a**) was interpreted as normal, without perfusion defects by the observers. cCTA (**b**) displayed as transverse section (*right upper panel*) and curved multiplanar reformat (*right middle panel*) shows high degree stenosis of the mid LAD caused by mixed calcified and noncalcified plaque (*arrows*), subsequently confirmed at invasive catheter angiography (*right lower panel*) and treated despite rather small perfusion defect but typical angina by stent placement. In retrospect the stress MPI study using the CT/SPECT system (*left lower panel* in **b**) shows a small apical area with reduced perfusion (*arrows*) which was initially not appreciated by the observers. Also shown are the attenuation-corrected (*upper row*) and uncorrected (*lower row*) studies in short, long horizontal, and long vertical axes. On fused CT/SPECT display (*left upper panel* in **b**), the perfusion defect can be more clearly visualized. *Upper middle image panel* shows the overlay of myocardial outlines generated at MPI (*color*) and at CT (*grayscale*) as a first step of the fusion process used for quality control

Additional findings

Incidental findings with potential impact on patient management were detected in four patients at CT. Two patients required follow-up for pulmonary nodules with 5- and 6-mm diameters, respectively [29]. One patient showed granulomatous lung disease. One patient presented with moderate pericardial effusion and intramyocardial bridging of the LAD.

Discussion

This feasibility study demonstrates that rapid assessment of coronary artery disease is possible with an integrated CT/SPECT system. Only one patient prematurely aborted the MPI examination due to back pain. Most interestingly, our study shows that only half of the patients with perfusion defects at routine clinical SPECT MPI had significant coronary artery stenosis at cCTA. Conversely, 16% of

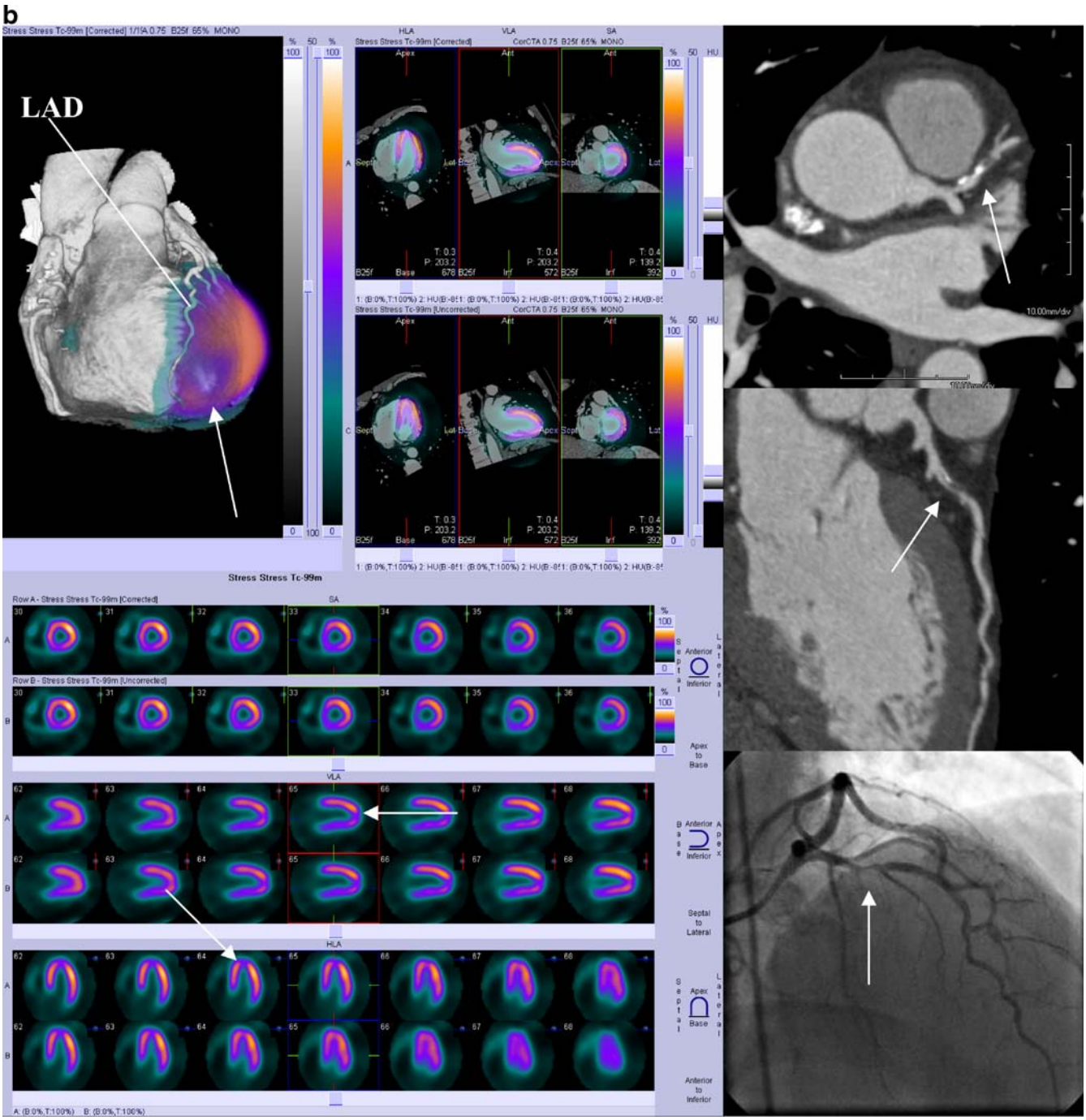

Fig. 4 (continued)

patients with a normal MPI study had significant stenosis at cCTA. A recent study illustrating the combined use of cCTA and MPI identified seven patients with significant stenosis out of 18 with normal perfusion studies (39%) [30]. Therefore, it can be stated that a single investigation currently fails to reliably meet clinical needs of all patients. These results are not unexpected in view of the previously described limitations in assigning perfusion defects to specific anatomic coronary lesions [31] and the limitation of cCTA in terms of evaluating smaller order vessels [32].

cCTA alone has been validated as a valuable tool for noninvasive morphologic assessment of the coronary arteries. Recent publications reported high sensitivities for cCTA in detecting significant (≥50%) stenosis ranging

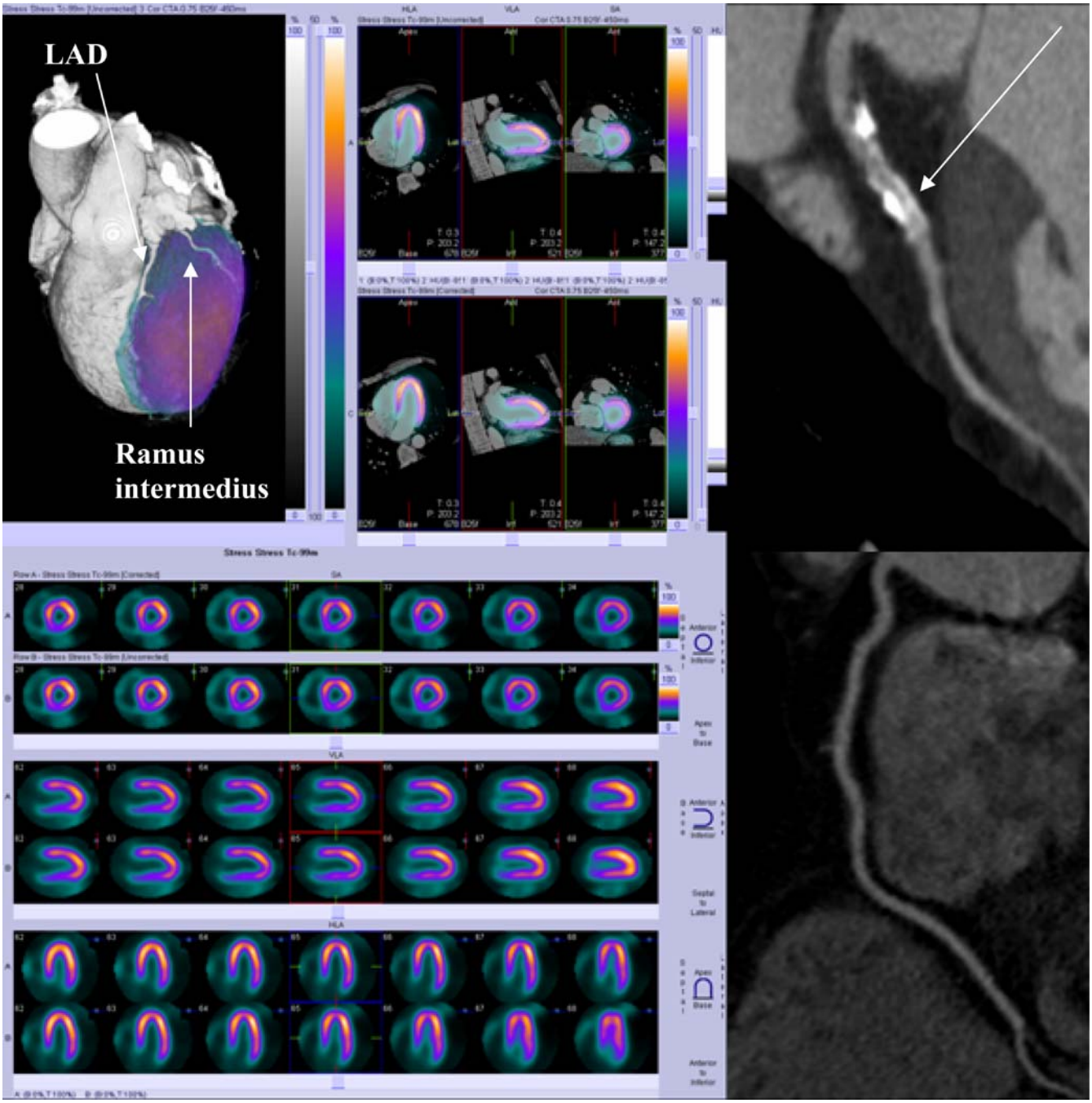

Fig. 5 CT/SPECT in a 54-year-old man (Table 2, patient 23) with known CAD, chronic, stable angina pectoris, and cardiovascular risk factors including hypertension and hyperlipidemia referred for myocardial perfusion imaging. cCTA displayed as curved multiplanar reformat (*right upper panel*) shows stenosis of the proximal LAD difficult to quantify due to severe calcification (*arrow*) and normal right coronary artery (*right lower panel*). Stress MPI study using the CT/SPECT system (*left lower panel*) shows normal perfusion. Patient was discharged (routine rest/stress MPI was also normal) and medical treatment was recommended. Also shown are the attenuation-corrected (*upper row*) and uncorrected (*lower row*) studies in short, long horizontal, and long vertical axes. Also, on fused CT/SPECT display (*left upper panel*) no perfusion defect can be visualized

from 94 to 99% compared with invasive coronary catheterization [3, 4, 33]. The most encouraging observation is the high negative predictive value of a normal cCTA study (97% with 64-slice CT on a per segment basis) [34]. This high negative predictive value suggests a potentially important role of noninvasive cCTA to reliably exclude severe CAD in the large population of patients with equivocal clinical presentation and/or imaging findings

Table 2 CT angiography results for the study patients and perfusion findings at routine rest/stress MPI and investigational stress MPI/cCTA fusion imaging

Patient	Stenosis at CTA	Routine MPI		Investigational MPI	
		Rest	Stress	Stress	Fusion
1	LAD mid 80%	Normal	Normal	Normal/X	X
2	None	Normal	Normal	N/A	N/A
3	None	Normal	Normal	Normal	Normal
4	RCA mid 100%, LAD mid 70%, LAD dist 70%, Cx dist 70%	I	I	I	I
5	None	Normal	Normal	Normal	Normal
6	LAD prox LIR	Normal	Normal	Normal	Normal
7	LAD mid 70%	Normal	Normal	Normal	Normal
8	None	Normal	Normal	Normal	Normal
9	None	Normal	Normal	Normal	Normal
10	None	Normal	X,A	X,A	X,A
11	LAD prox 40%	Normal	Normal	Normal	Normal
12	None	Normal	Normal	Normal	Normal
13	CABG RCA dist 70%, CABG Cx 100%	I,L	I,L	I,L	I,L
14	LAD prox 40%, LAD mid 40%	Normal	Normal	Normal	Normal
15	None	Normal	Normal	Normal	Normal
16	None	Normal	Normal	Normal	Normal
17	D1 40%	Normal	I,S	I,S	I,S
18	None	Normal	Normal	I,A	I
19	None	Normal	Normal	Normal	Normal
20	None	Normal	Normal	Normal	Normal
21	LAD mid 50–60%	Normal	I	I	I
22	None	Normal	Normal	Normal	Normal
23	LAD mid 50–60%	Normal	Normal	Normal	Normal
24	None	Normal	A	A	A
25	None	Normal	Normal	Normal	Normal

Patient 2 aborted investigational MPI. In patient 1 apical defect at investigational MPI was seen in retrospect (see Fig. 4)
N/A not applicable, *LAD* left anterior descending, *CABG* coronary artery bypass graft, *RCA* right coronary artery, *Cx* circumflex artery, *D1* 1st diagonal branch, *LIR* luminal irregularities, *A* anterior, *I* inferior, *S* septal, *X* apex, *L* lateral

(e.g., MPI). These individuals currently undergo a costly invasive evaluation for exclusion of a relatively low likelihood of stenotic CAD. One major limitation of cCTA, regardless of the instrument generation, is the presence of calcification within the coronary arteries. The accuracy for grading stenosis is limited by the amount of calcification in the vessel wall. cCTA radiation exposure should be considered, especially if repeat evaluation of CAD is required. Techniques such as tube current modulation to reduce radiation dose are recommended [35] and were used in this study. Additional limitations, such as the need for a regular heart rhythm and a relatively low heart rate (<65 bpm) are overcome with new instrument generations such as dual-source CT.

Although cCTA can reliably exclude coronary artery stenosis, its potential to evaluate the hemodynamic significance of detected lesions is limited. In order to identify the significance of lesions possibly requiring intervention, MPI is usually performed after cCTA. In contrast, cCTA is performed after MPI when perfusion results are equivocal. In addition to hemodynamic information, MPI adds important prognostic value concerning cardiac mortality and myocardial infarction enabling risk-stratification of patients with CAD or following MI. MPI is the most powerful predictor of outcome in patients with coronary artery disease, even exceeding coronary angiography [36]. Normal MPI implies a cardiac mortality of less than 1% per year [37]. However, MPI has some inherent limitations due to several pitfalls and artefacts. Patient-related artefacts may arise from tissue attenuation (e.g., breast attenuation). Artefacts and pitfalls originating from the target organ include left bundle branch block, hypertrophic cardiomyopathy, HOCM, and balanced ischemia. Common technical problems include patient motion and incorrect ECG gating [38].

The combination of morphologic and functional imaging with MPI and invasive coronary catheterization is an essential component of current practice. Once a stenosis is categorized as significant at MPI, patients may be referred for an interventional procedure. Frequently, patients may undergo coronary catheterization twice with all risks related to an invasive procedure. More recent approaches suggest the use of cCTA for stenosis detection instead of invasive coronary catheterization. For image interpretation, a side-by-side analysis of studies has been shown to be useful in the detection of hemodynamically relevant coronary artery stenosis [30]. However, in order to optimize the clinical value of these modalities, integration of anatomic with hemodynamic information is desirable—most intuitively displayed by 3D image fusion. Gaemperli at al. [20] demonstrated that in one third of patients undergoing combined MPI SPECT and CTA, fused images provided added diagnostic information about the pathophysiologic lesion severity in comparison to isolated analysis. These results are in agreement with a previously reported evaluation of a hybrid device with improvement of both specificity and positive predictive value [10]. In our small cohort one additional patient with a significant stenosis and perfusion defect was identified at image fusion.

There are several limitations of this study. The investigation was designed as a feasibility study evaluating an investigational integrated CT/SPECT system. Patients were consecutively enrolled in the study regardless of their likelihood of having coronary disease. This resulted in a large number of "normals" at both CTA and MPI.

Two patients had prior coronary artery bypass grafts with limited stenosis evaluation at the distal anastomosis. Also, blooming artefacts from metallic stent struts (seven patients) interfered with the assessment of in-stent stenosis.

cCTA results were not routinely confirmed by invasive coronary catheterization as the reference standard in the great majority of patients; invasive coronary catheterization was only performed in four patients. Furthermore, MPI rest imaging was not performed in the research setting but will be part of the workup if hybrid imaging emerges as a routine examination. Potential decay of sestamibi between clinical and research imaging can be neglected since the research data acquisition began 30 min after the completion of the clinical study. Decay-corrected biological half-life for sestamibi has been shown to be 680±45 min and 1,045±56 min for normal and ischemic myocardium, respectively [39].

Despite these limitations a decrease of the incidence of false positive MPI findings can be expected by an integrated assessment since only half of the patients with perfusion defects had significant stenosis. Secondly, there might be findings beyond a "normal" MPI study. In four patients who were normal at MPI noncalcified plaque was found on cCTA. Three out of 19 patients with normal perfusion on MPI had other findings including myocardial bridging, granulomatous lung disease, and incidental pulmonary nodules.

One may hypothesize that the combination of stenosis detection and evaluation of perfusion enabled by the hybrid CT/SPECT may facilitate a more comprehensive assessment of coronary heart disease in a safe and less time-consuming manner than with stand-alone modalities. Information about lesion morphology at CTA (e.g., length of stenosis, amount and character of calcification-eccentric, calcified, noncalcified, exact localization of bypass graft ostia) may aid in planning percutaneous intervention. It may also be expected that combined imaging could be of value to correctly identify the culprit vessel in cases of nonstandard coronary anatomy.

Moreover, both a negative cCTA study and a negative MPI study may further increase the negative predictive value for the exclusion of coronary artery disease by noninvasive methods.

Attenuation correction techniques represent a significant advance in myocardial perfusion imaging and were used in this study. With the hybrid imaging system, attenuation correction can be performed using the calcium scoring examination with minimal effort [40]. The advantage of a hybrid system over stand-alone instruments must be evaluated in further studies. However, it can be hypothesized that a hybrid system promises faster (one location) and more accurate evaluation of CAD as no repositioning of the patient is required and attenuation correction can be accomplished via calcium scoring with immediate implementation in the SPECT imaging component, and images can be directly combined during display and analysis without the need for complex image fusion algorithms.

In conclusion, the combined assessment of coronary anatomy and myocardial perfusion with a hybrid CT/SPECT system with 3D image fusion is feasible and may facilitate the detection of coronary artery lesions, thus improving the accuracy of CAD diagnosis.

References

1. Fine JJ, Hopkins CB, Ruff N et al (2006) Comparison of accuracy of 64-slice cardiovascular computed tomography with coronary angiography in patients with suspected coronary artery disease. Am J Cardiol 97:173–174
2. Leber AW, Knez A, von Ziegler F et al (2005) Quantification of obstructive and nonobstructive coronary lesions by 64-slice computed tomography: a comparative study with quantitative coronary angiography and intravascular ultrasound. J Am Coll Cardiol 46:147–154
3. Leschka S, Alkadhi H, Plass A et al (2005) Accuracy of MSCT coronary angiography with 64-slice technology: first experience. Eur Heart J 26:1482–1487
4. Mollet NR, Cademartiri F, van Mieghem CA et al (2005) High-resolution spiral computed tomography coronary angiography in patients referred for diagnostic conventional coronary angiography. Circulation 112:2318–2323
5. Pugliese F, Mollet NR, Runza G et al (2006) Diagnostic accuracy of non-invasive 64-slice CT coronary angiography in patients with stable angina pectoris. Eur Radiol 16:575–582
6. Raff GL, Gallagher MJ, O'Neill WW et al (2005) Diagnostic accuracy of non-invasive coronary angiography using 64-slice spiral computed tomography. J Am Coll Cardiol 46:552–557
7. Ropers D, Rixe J, Anders K et al (2006) Usefulness of multidetector row spiral computed tomography with 64-×0.6-mm collimation and 330-ms rotation for the noninvasive detection of significant coronary artery stenoses. Am J Cardiol 97:343–348
8. Dowe DA (2007) The case in favor of screening for coronary artery disease with coronary CT angiography. J Am Coll Radiol 4:289–294
9. Di Carli MF, Hachamovitch R (2007) New technology for noninvasive evaluation of coronary artery disease. Circulation 115:1464–1480
10. Rispler S, Keidar Z, Ghersin E et al (2007) Integrated single-photon emission computed tomography and computed tomography coronary angiography for the assessment of hemodynamically significant coronary artery lesions. J Am Coll Cardiol 49:1059–1067
11. Schuijf JD, Wijns W, Jukema JW et al (2006) Relationship between noninvasive coronary angiography with multislice computed tomography and myocardial perfusion imaging. J Am Coll Cardiol 48:2508–2514
12. Berman DS, Hachamovitch R, Kiat H et al (1995) Incremental value of prognostic testing in patients with known or suspected ischemic heart disease: a basis for optimal utilization of exercise technetium-99 m sestamibi myocardial perfusion single-photon emission computed tomography. J Am Coll Cardiol 26:639–647
13. Hachamovitch R, Berman DS, Kiat H et al (1996) Exercise myocardial perfusion SPECT in patients without known coronary artery disease: incremental prognostic value and use in risk stratification. Circulation 93:905–914
14. Hachamovitch R, Hayes SW, Friedman JD et al (2003) Comparison of the short-term survival benefit associated with revascularization compared with medical therapy in patients with no prior coronary artery disease undergoing stress myocardial perfusion single photon emission computed tomography. Circulation 107:2900–2907
15. Klocke FJ, Baird MG, Lorell BH et al (2003) ACC/AHA/ASNC guidelines for the clinical use of cardiac radionuclide imaging-executive summary: a report of the American College of Cardiology/American Heart Association Task Force on Practice Guidelines (ACC/AHA/ASNC Committee to Revise the 1995 Guidelines for the Clinical Use of Cardiac Radionuclide Imaging). J Am Coll Cardiol 42:1318–1333
16. O'Keefe JH Jr., Bateman TM, Ligon RW et al (1998) Outcome of medical versus invasive treatment strategies for non-high-risk ischemic heart disease. J Nucl Cardiol 5:28–33
17. IMV Medical Information Division (2003) Nuclear medicine market summary report. IMV, Des Plaines, IL,USA
18. Berman DS, Hachamovitch R, Shaw LJ et al (2006) Roles of nuclear cardiology, cardiac computed tomography, and cardiac magnetic resonance: assessment of patients with suspected coronary artery disease. J Nucl Med 47:74–82
19. Russell RR 3rd, Zaret BL (2006) Nuclear cardiology: present and future. Curr Probl Cardiol 31:557–629
20. Gaemperli O, Schepis T, Valenta I et al (2007) Cardiac image fusion from stand-alone SPECT and CT: clinical experience. J Nucl Med 48:696–703
21. Nakaura T, Utsunomiya D, Shiraishi S et al (2005) Three-dimensional cardiac image fusion using new CT angiography and SPECT methods. AJR Am J Roentgenol 185:1554–1557
22. Faber TL, Santana CA, Garcia EV et al (2004) Three-dimensional fusion of coronary arteries with myocardial perfusion distributions: clinical validation. J Nucl Med 45:745–753
23. Hansen CL, Goldstein RA, Berman DS et al (2006) Myocardial perfusion and function single photon emission computed tomography. J Nucl Cardiol 13:e97–e120
24. Fleischmann S, Koepfli P, Namdar M et al (2004) Gated (99 m)Tc-tetrofosmin SPECT for discriminating infarct from artifact in fixed myocardial perfusion defects. J Nucl Med 45:754–759
25. Cerqueira MD, Weissman NJ, Dilsizian V et al (2002) Standardized myocardial segmentation and nomenclature for tomographic imaging of the heart: a statement for healthcare professionals from the Cardiac Imaging Committee of the Council on Clinical Cardiology of the American Heart Association. Circulation 105:539–542
26. Flohr T, Ohnesorge B (2001) Heart rate adaptive optimization of spatial and temporal resolution for electrocardiogram-gated multislice spiral CT of the heart. J Comput Assist Tomogr 25:907–923
27. Flohr T, Ohnesorge B, Bruder H et al (2003) Image reconstruction and performance evaluation for ECG-gated spiral scanning with a 16-slice CT system. Med Phys 30:2650–2662
28. Ohnesorge B, Flohr T, Becker C et al (2000) Cardiac imaging with rapid, retrospective ECG synchronized multilevel spiral CT. Radiologe 40:111–117
29. Beigelman-Aubry C, Hill C, Grenier PA (2007) Management of an incidentally discovered pulmonary nodule. Eur Radiol 17:449–466
30. Hacker M, Jakobs T, Hack N et al (2007) Combined use of 64-slice computed tomography angiography and gated myocardial perfusion SPECT for the detection of functionally relevant coronary artery stenoses. First results in a clinical setting concerning patients with stable angina. Nuklearmedizin 46:29–35

31. Schindler TH, Magosaki N, Jeserich M et al (1999) Fusion imaging: combined visualization of 3D reconstructed coronary artery tree and 3D myocardial scintigraphic image in coronary artery disease. Int J Card Imaging 15:357–368 discussion 369–370
32. Herzog C, Zwerner PL, Doll JR et al (2007) Significant coronary artery stenosis: comparison on per-patient and per-vessel or per-segment basis at 64-section CT angiography. Radiology 244:112–120
33. Nieman K, Cademartiri F, Lemos PA et al (2002) Reliable noninvasive coronary angiography with fast submillimeter multislice spiral computed tomography. Circulation 106:2051–2054
34. Nikolaou K, Knez A, Rist C et al (2006) Accuracy of 64-MDCT in the diagnosis of ischemic heart disease. AJR Am J Roentgenol 187:111–117
35. Jakobs TF, Becker CR, Ohnesorge B et al (2002) Multislice helical CT of the heart with retrospective ECG gating: reduction of radiation exposure by ECG-controlled tube current modulation. Eur Radiol 12:1081–1086
36. Mowatt G, Brazzelli M, Gemmell H et al (2005) Systematic review of the prognostic effectiveness of SPECT myocardial perfusion scintigraphy in patients with suspected or known coronary artery disease and following myocardial infarction. Nucl Med Commun 26:217–229
37. Metz LD, Beattie M, Hom R et al (2007) The prognostic value of normal exercise myocardial perfusion imaging and exercise echocardiography: a meta-analysis. J Am Coll Cardiol 49:227–237
38. Burrell S, MacDonald A (2006) Artifacts and pitfalls in myocardial perfusion imaging. J Nucl Med Technol 34:193–211
39. Munch G, Neverve J, Matsunari I et al (1997) Myocardial technetium-99 m-tetrofosmin and technetium-99 m-sestamibi kinetics in normal subjects and patients with coronary artery disease. J Nucl Med 38:428–432
40. Hendel RC, Corbett JR, Cullom SJ et al (2002) The value and practice of attenuation correction for myocardial perfusion SPECT imaging: a joint position statement from the American Society of Nuclear Cardiology and the Society of Nuclear Medicine. J Nucl Cardiol 9:135–143